

## Statistics of wave crests from models vs. measurements

### Marc Prevosto

IFREMER - Centre de BREST  
BP 70  
29280 Plouzané  
France  
Fax: +33 (0)2-98-22-46-50  
Email: marc.prevosto@ifremer.fr

### George Z. Forristall

Shell Global Solutions International, B.V.  
Volmerlaan 8  
2280AB Rijswijk  
The Netherlands

### ABSTRACT

The analysis phase of the Wave Crest Sensor Intercomparison Study (WACSIS) focussed on the interpretation of the wave data collected by the project during the winter of 1997-98. Many aspects of wave statistics have been studied, but the main emphasis has been on crest height distributions, and recommendations for crest heights to be used in air gap calculations.

In this paper we first describe comparisons of the crest height distributions derived from the sensors (radars, wave staffs, laser) and from simulations based on 3D second order irregular wave models. These comparisons permit us to make conclusions on the quality of these models and to qualify the ability of some sensors to measure the crest heights accurately. In the second part two new parametric models of the crest height distributions are discussed and their superiority to standard parametric models is demonstrated.

### INTRODUCTION

**In-situ measurements.** The statistics of wave crests for specific site studies have generally been based on *in-situ* measurements (North-Sea and Gulf of Mexico oil fields). The incomparably great quality of a measurement is that it includes all the physical phenomena, but unfortunately also those which corrupt the actual observation of waves (mooring behavior and transfer function for buoys, fouling effect for plunged or underwater probes, sea foam or spray effect). To this list will be added the problems of spatial integration, calibration and data transformation and transmission. Wave instruments furnish point measurements and so it can take a long time to build

reliable statistics. The instrumentation is also expensive, making the cost and duration of a measurement program incompatible with the constraints of the project.

**Models.** The methodologies to furnish statistics of crest height for individual sea states starting from spectral information are of different kinds. They can be based on Monte Carlo techniques and development of simulators or derived from theoretical considerations such as the Transformed Gaussian process method (Rychlik *et al.* (1997)) or First Order Reliability Method (FORM) (Tromans and Taylor (1998), Tromans, (2002)). But independent of the methodology, the answers will depend on the model of irregular gravity waves taken as starting point. It is well known that linear models do not reproduce sufficiently accurately the crest heights in steep sea states, so more complicated models have to be considered to take into account the strong effect of the nonlinearities on the crest amplitudes, e.g. the Hybrid Model or the Creamer-transformation. The simplest model which includes nonlinearity and wave spreading is the second order model for irregular seas.

**Models vs. measurements.** In this paper, after some considerations on the simulation parameters of the 2nd order models, we compare the crest statistics obtained from these models with those from measurements of the WACSIS project (Forristall *et al.* 2002). This comparison has permitted us to validate the 2nd order models for crest heights in the sea conditions encountered during the measurement campaign. Moreover, comparisons with measurements coming from six different crest height sensors have supplied a way of investigating discrepancies between the sensors.

In the second part of the paper, we compare classical and new parametric models of the cumulative distribution of crest heights based on 2nd order models which have been proposed as practical tools for engineers. This comparison shows the superiority of the two new models proposed by the authors, which, in addition, take into account the 3D structure of the waves.

## SIMULATION METHODS - EFFECT OF SIMULATION PARAMETERS

In order to compute the crest statistics given by second order models of waves and then fit parameterized models of crest heights, we have used simulation methods for the elevation of the free surface. The formulas are based on the irregular wave version of the second order Stokes expansion. They were calculated for infinite water depth by Longuet-Higgins (1963) and the calculations were extended to intermediate water depth by Sharma and Dean (1979).

### Models of wave surface elevation

The nonlinear model of the elevation process is the superposition of two processes:

$$\eta(t) = \eta_1(t) + \eta_2(t) \quad (1)$$

The first order (linear) part  $\eta_1(t)$  of this model is a directional Gaussian process (superposition of Airy waves in different directions of propagation with random phases and amplitudes):

**Linear part.** The linear part is defined as:

$$\eta_1(t) = \sum_{\theta, f} b(\theta, f) \sin(2\pi f t) + c(\theta, f) \cos(2\pi f t) \quad (2)$$

with b and c Gaussian random variables defined by

$$\begin{aligned} \mathbf{IE}(b(\theta, f)^2) &= \mathbf{IE}(c(\theta, f)^2) = S(\theta, f) d\theta df \\ \mathbf{IE}(b(\theta_i, f_j) c(\theta_k, f_l)) &= 0 \end{aligned} \quad (3)$$

where  $S(\theta, f)$  is the directional spectral density.  $\eta_1(t)$  can be rewritten

$$\eta_1(t) = \sum_{\theta, f} a(\theta, f) \sin(2\pi f t + \phi(\theta, f)) \quad (4)$$

with now  $a(\theta, f)$  a Rayleigh random variable and  $\phi(\theta, f)$  a uniform random variable in  $[-\pi, \pi]$ , with

$$\mathbf{IE}(a(\theta, f)^2) = 2S(\theta, f) d\theta df \quad (5)$$

and  $a(\theta_i, f_j)$ ,  $\phi(\theta_k, f_l)$  independent variables.

Using Eqs. (2) & (3) or Eqs. (4) & (5) includes the proper variability of the spectral amplitudes and so of the Gaussian process

**2nd order directional - 3D.** The 2nd order Stokes expansion based on this linear part is

$$\begin{aligned} \eta_2(t) &= \sum_{\theta_i, f_j, \theta_k, f_l} a_{ij} a_{kl} T^D(\theta_i, f_j, \theta_k, f_l) \cos(2\pi(f_j - f_l) + (\phi_{ij} - \phi_{kl})) \\ &+ \sum_{\theta_i, f_j, \theta_k, f_l} a_{ij} a_{kl} T^S(\theta_i, f_j, \theta_k, f_l) \cos(2\pi(f_j + f_l) + (\phi_{ij} + \phi_{kl})) \quad (6) \\ &- c_{\eta_2} \end{aligned}$$

where  $a_{ij}$  (resp.  $\phi_{ij}$ ) denotes  $a(\theta_i, f_j)$  (resp.  $\phi(\theta_i, f_j)$ ) and  $c_{\eta_2}$  is a constant to ensure that  $\mathbf{IE}(\eta_2(t)) = 0$ .

The two 2nd order transfer functions  $T^S$  and  $T^D$  of course depend of the water depth (Sharma and Dean (1979), Prevosto (2000)).

**2nd order uni-directional - 2D.** If we consider a uni-directional wave train in which all the components propagate in the same direction, we obtain, of course, the same linear part of the elevation, but a different second order part.

$$\eta_1(t) = \sum_{\theta, f} a(\theta, f) \sin(2\pi f t + \phi(\theta, f)) = \sum_f a_u(f) \sin(2\pi f t + \phi_u(f)) \quad (7)$$

$$\begin{aligned} \eta_2(t) &= \sum_{f_j, f_l} a_u(f_j) a_u(f_l) T_u^D(f_j, f_l) \cos(2\pi(f_j - f_l) + (\phi_u(f_j) - \phi_u(f_l))) \\ &+ \sum_{f_j, f_l} a_u(f_j) a_u(f_l) T_u^S(f_j, f_l) \cos(2\pi(f_j + f_l) + (\phi_u(f_j) + \phi_u(f_l))) \quad (8) \\ &- c_{\eta_2} \end{aligned}$$

**Non-linear narrowband - 2D.** A simplified model of 2nd order uni-directional waves is obtained if the spectral density is sufficiently narrow to consider the 2nd order transfer functions as constant around a frequency  $f_m$ . In this case,  $T_u^D(f_j, f_l)$  (resp.  $T_u^S(f_j, f_l)$ ) are considered constant and equal to  $T_{nb}^D(f_m)$ , (resp.  $T_{nb}^S(f_m)$ ), with

$$T_{nb}^D(f_m) = \lim_{\substack{f_j \rightarrow f_m \\ f_l \rightarrow f_m}} T_u^D(f_j, f_l) \quad , \quad T_{nb}^S(f_m) = \lim_{\substack{f_j \rightarrow f_m \\ f_l \rightarrow f_m}} T_u^S(f_j, f_l) \quad (9)$$

which gives for the second order part

$$\begin{aligned} \eta_2(t) &= T_{nb}^D(f_m) \sum_{f_j, f_l} a_u(f_j) a_u(f_l) \cos(2\pi(f_j - f_l) + (\phi_u(f_j) - \phi_u(f_l))) \\ &+ T_{nb}^S(f_m) \sum_{f_j, f_l} a_u(f_j) a_u(f_l) \cos(2\pi(f_j + f_l) + (\phi_u(f_j) + \phi_u(f_l))) \quad (10) \\ &- T_{nb}^D(f_m) \sum_f a_u^2(f) \end{aligned}$$

If  $\eta_1(t)$  is considered as a product of an amplitude and a phase time function,  $\eta_1(t) = A(t) \cos(\Omega(t))$ , where the amplitude and instantaneous frequency are slowly varying, the unidirectional narrowband second order part becomes

$$\eta_2(t) = -\frac{1}{8} H_s^2 T_{nb}^D(f_m) + T_{nb}^D(f_m) A^2(t) + T_{nb}^S(f_m) A^2(t) \cos(2\Omega(t)) \quad (11)$$

The formulas for  $T_{nb}^D$  and  $T_{nb}^S$  are given in Prevosto *et al.* (2000).

## Simulation method

The simulation method consists of calculating the formulas of the 2nd order transfer function, drawing the random variables  $b(\theta, f)$  and  $c(\theta, f)$  from the linear part (Eq. (2)) and calculating the 2nd order part taking into account all the interactions between the components. The  $b$  and  $c$  coefficients depend on the directional spectral density of the sea-states (Eq. (3)).

**Directional spectrum.** A Waverider was used during the WACSIS campaign to furnish the directional information. Measurements from a directional buoy do not completely describe the directional spectrum. To complete this information we chose a  $\cos^{2s}$  classical shape of directional spreading.

$$\begin{cases} S(f, \theta) = S(f)H(f, \theta) \\ H(f, \theta) = A(s(f))\cos^{2s(f)}\left(\frac{\theta - \bar{\theta}(f)}{2}\right) \end{cases} \quad (12)$$

The Waverider furnished the point spectrum  $S(f)$  and the variations with frequency of the mean direction  $\bar{\theta}(f)$  and of the spreading coefficient  $s(f)$ .

**Truncation of the spectrum.** As it is explained by Chen and Zhang (1994), the non-linear interactions between long and very short waves are very badly calculated with a Stokes expansion and for better accuracy they introduce a modulated wave-mode approach. This approach results in a so-called hybrid model (Zhang *et al.* 1996). This approach may be necessary in the computation of the kinematics in the crest, but in the case of free-surface elevation, a simpler method can be used to avoid the poor convergence of the Stokes expansion of the non-linear interactions between long and short waves. It consists merely in a truncation of the spectral density, thus removing very long and short waves from the nonlinear interactions.

## Effect of simulation parameters

It is necessary to understand as well as possible the effects on the simulation of the angular and frequency discretization, the frequency truncation, the water depth and the source of the input spectrum. The accuracy of the simulation will depend on these parameters which have to be determined carefully to avoid bias in the comparison between the simulations and the measurements.

**Discretization of the directional spectrum.** To study the best number of directional sectors, the interval  $[-\pi, +\pi]$  has been regularly discretized into 255, 127, 63, 31, 15, 7, 3, or 1 sectors. The case with 1 sector corresponds to the 2D case. The comparison of the crest height statistics for these different discretizations shows that, for a typical sea state at the WACSIS site, 31 sectors are needed to accurately simulate the effect of spreading on the nonlinear interactions.

**Frequency truncation.** The effect of frequency truncation is quite different for the 2D and the 3D case. Four percentages of

truncation have been tested: 1%, 2%, 5%, 10%. The percentages indicated correspond to the amount of energy removed from each side of the peak frequency, starting from the lowest and the highest frequencies.

We observed that mainly in the 2D case the computation without truncation generates waves with unphysical shapes due, as said previously, to the very bad convergence of the short-long wave interactions. In removing 1% energy of the shorter waves and 1% energy of the longer waves we remove a very small part of the nonlinear interactions but avoid the relatively large error of convergence of their interactions (especially for the 2D case). When the amount of truncation is increased, removing a greater part of the nonlinear interactions, the crest heights statistics are significantly modified.

In fact in the actual sea states, either we are close to a 2D situation, which corresponds to long-crested waves (swell), and in this case the spectrum is relatively narrow and so the problem of short-long waves interactions is avoided, or we are in a short-crested waves situation (wind sea), clearly 3D, where the short-long waves interactions present due to a broader spectrum do not seem to create real problems. Thus, the frequency truncation does not seem so critical in practice, but a rate of 1% has been used for all the simulations reported in this paper.

**Water depth.** When the waves propagate on intermediate water depth (in fact it is the dimensionless ratio of water depth to wavelength which is critical) the kinematics and the wave elevation are modified. As can be seen from the second order transfer functions, the nonlinear interactions are also modified by a change in the water depth. At the WACSIS site the tide and the storm surge induced variations of the water depth in the range 16.4-20.0 m.

The effect on the crest height statistics obtained by simulation is significant, but again the amplitude of the effect is quite different in the 2D case and in the 3D case. The modifications are quite important in the 3D case, which corresponds to the actual cases, and so an accuracy of the order of 0.1 m. is necessary (at the WACSIS site and for the average wavelengths encountered) in the mean water level to accurately calculate the crest height statistics.

**Point spectrum.** The primary information for the simulation is the directional spectrum. So it is important to know if the crest height statistics are sensitive to the type of sensor which furnishes the point spectrum. As it is well known, a buoy of free-floating type, due to the principle of measurement, does not measure bounded waves in infinite depth, and only partially (theoretically) in finite depth. Other sensors like lasers or wave staffs measure the bounded waves well. As the spectral density used in our models is considered as being the spectrum of the free waves (Eq. (2)), if the spectrum used comes from a laser or a wave staff and so contains also the energy of the bounded waves, then there is an inconsistency in the calculations.

The comparison of the crest height statistics however showed that the weak energy of the bounded waves treated as energy of free waves when using the spectra coming from a Baylor Wave Staff or a EMI Laser has no significant effect on the simulations.

## COMPARISON MEASUREMENTS-SIMULATION

The problem which now is posed is to know if the simulations furnish crest statistics comparable to the measurements. And, as the different sensors used during the WACSIS project give different crest statistics, a second issue should be answered: do the simulations validate the results obtained by one or more sensors? We recall here the six sensors analysed in this study: EMI Laser, Baylor Wave Staff, Marex radar, Saab radar, Vlissingen step gauge, Waverider (see Forristall (2002) for more details). For the comparisons reported hereafter, all the measurements have been filtered at 0.64 Hz using a boxcar filter. This filtering is done for two reasons. First, the power spectra from the sensors indicated (Forristall *et al.* 2002) that the measurements are very likely to be contaminated by noise above this frequency. Secondly, the Waverider spectra used for simulations give energy of the linear part only up to 0.64Hz.

It is difficult to learn much from comparisons of crest height statistics for individual sea states due to the combined effects of the short duration of the series (~20 min.), the different locations of the sensors and the great variability in time and space of the wave field in wind sea conditions. Therefore two means of combining data from different hours have been used to compare the crest height statistics:

**Crest height ratios.** By combining several hours of data with similar wave heights we can eliminate some of the sampling variability in single data records while still being able to see variations due to different ranges of wave heights. If the waves could be described by linear theory, the crest heights would follow the Rayleigh distribution given by

$$P(C > c) = \exp\left(-8 \frac{c^2}{H_s^2}\right) \quad (13)$$

where  $C$  is the crest height,  $H_s = 4\sqrt{m_0}$  is the significant wave height and  $m_0$  is the variance of the wave spectrum. We can get a clear picture of the effect of the nonlinearities on the crest heights by plotting the ratio of the measured crest height divided by the height predicted by the Rayleigh distribution against the probability that the measured crest height is exceeded. Since the crest height ratios are normalized by the significant wave height of the sensor during each record, there are no difficulties with combining records with different significant wave heights or with different sensors measuring slightly different significant wave heights during a sea state.

**Crests all-over campaign.** The analysis of the waves accumulated over all of the campaign furnishes another precise tool of comparison. The empirical number of exceedances is

roughly calculated on the samples as

$$N(C > c) = n - \sum_{i=1}^n \mathbf{1}_{]-\infty, c]}(c_i) \quad (14)$$

where  $n$  is the total number of crests observed during the campaign.

This number of exceedances gives information on the empirical long (campaign) term statistics. In each figure showing these statistics, the approximate number of crests  $n$  will be indicated in the abscissa caption along with the number of 20 min. time series used to build the sample.

Due to the poor sampling of severe sea states in the EMI Laser data base, and to not degrade the comparisons with other instruments, we have analyzed separately two data bases, one without the EMI Laser (called MSVB (Marex radar, Saab radar, Vlissingen step gauge, Baylor wave staff) corresponding to about 60 (resp. 700) crests higher than 4 (resp. 3) meters and a second one with only the EMI Laser and the Baylor Wave Staff (called EB) corresponding to about 20 (resp. 300) crests higher than 4 (resp. 3) meters.

## Comparisons of crest height ratios

Figures 1-4 show the crest height ratios of all of the data with significant wave heights higher than 3 m in increments of 0.5 m. The simulations are from 1000 repetitions using the directional wave spectrum measured by the Waverider.

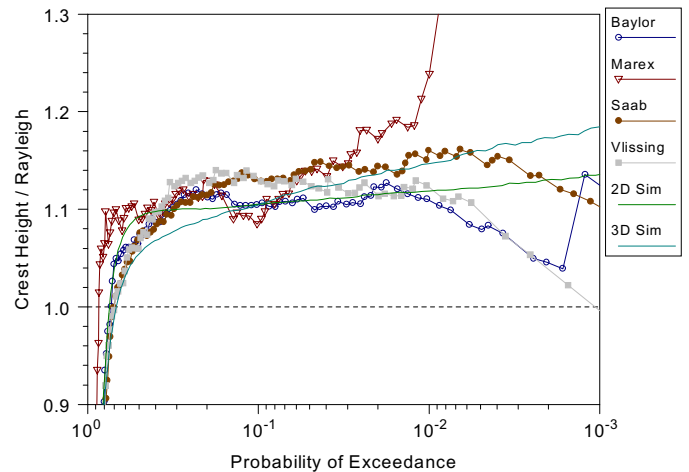


**Figure 1. Crest height ratios,  $H_s$  over 4.5 m.**

For significant wave heights greater than 3.0 m, the filtered measurements divide into two groups, with the measurements from the Saab and Marex radars being slightly higher than those from the Baylor, EMI, and Vlissingen instruments. Even after the filtering, there are some large noise spikes in the Marex data. The Baylor, EMI and Vlissingen instruments agree very closely with the simulations while the radars are a few percent higher. The three dimensional (directionally spread) simulations give slightly higher crest heights than the two dimensional

simulations in these conditions.

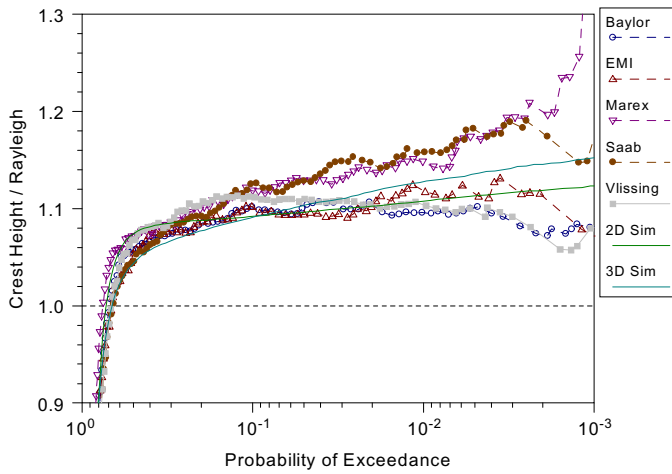


**Figure 2. Crest height ratios,  $4.0 < H_s < 4.5\text{m}$ .**

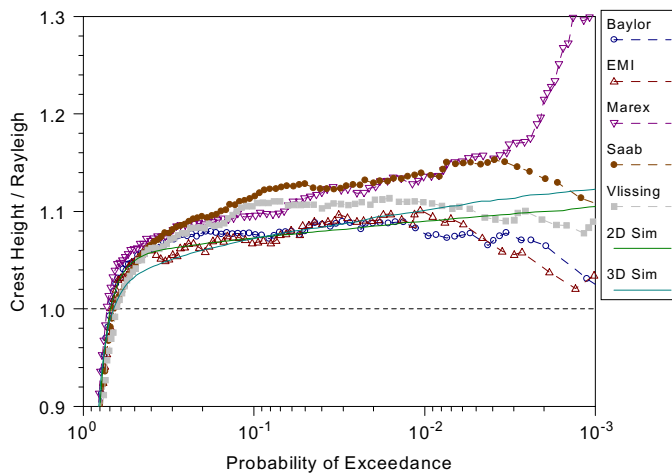


**Figure 3. Crest height ratios,  $3.5 < H_s < 4.0\text{m}$ .**

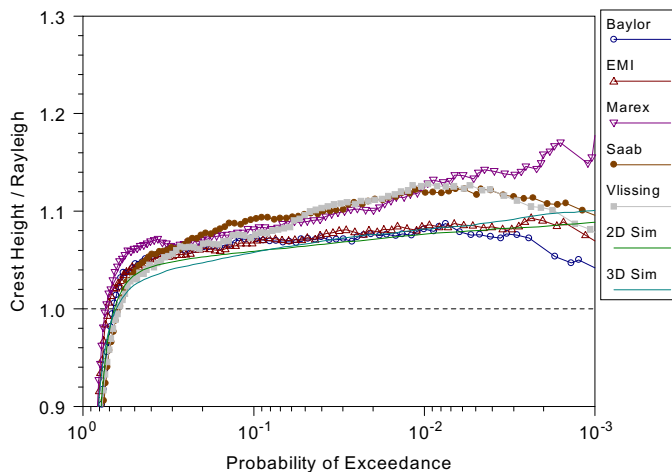


**Figure 4. Crest height ratios,  $3.0 < H_s < 3.5\text{m}$ .**

For the lower wave height ranges (not plotted here), the measurements are grouped closer together with a mean just slightly higher than the simulations. For the lowest waves, the

Vlissingen step gauge is noticeably higher than the other instruments, presumably because of its discrete resolution.

### Crest height distribution all-over campaign

Using the 3D irregular wave model, 1000 realizations of the WACSIS campaign have been simulated by simulating for each 17 min. sea state of the WACSIS data base 1000 time series. This has permitted us to calculate for crests over the whole campaign a median number of exceedances and the 95% confidence interval of the number of exceedances. The median corresponding to a linear irregular wave model has been also calculated as comparison.

The results of these simulations have been compared to the number of exceedances obtained from the measurements. In the MSVB data base (Fig. 5), the Vlissingen step gauge and the Baylor wave staff give very close results and inside the confidence interval. In the EB data base (Fig. 6), the EMI laser and the Baylor wave staff give again close results inside the confidence interval. The simulations are in very good agreement with these three sensors. Compared to these three sensors, the Saab radar is at the border of the confidence interval, slightly overestimating the crest levels compared to the simulations. The spikes in the measurements put Marex radar out of the confidence intervals.

As is well known, the buoy gives crest height statistics very close to those obtained from the linear hypothesis in deep water. When looking at the results Fig. 7 obtained from the Waverider, it is clearly also the case in the intermediate water depths of the WACSIS site.

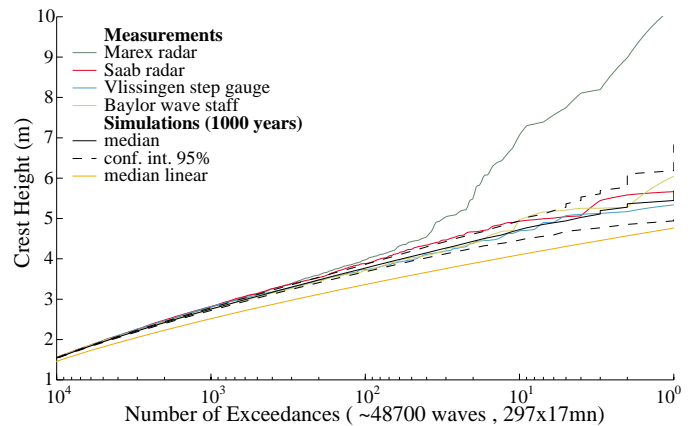


**Figure 5. MSVB Crest heights all-over campaign**

### Measurements vs. Simulation - Conclusion

Simulations of the wave elevation with a second order irregular 3D model give statistics of crest height similar to three of the sensors when we consider only wave components up to 0.64 Hz. The Saab and the Marex radars gave crest heights somewhat higher than the simulations even after the measurements were filtered. It is possible that part of the reason

for this difference is a combination of the hydrodynamics of short waves riding on long waves and the way that radar sensors respond to the short waves. The conventional perturbation expansion which we have used for our simulations is not accurate when high frequency waves are carried far from  $z = 0$  by the large low frequency waves. For short waves riding on long waves, it is more appropriate to expand the free surface boundary conditions at the long wave surface rather than at the undisturbed surface as discussed by Zhang *et al.* (1999).

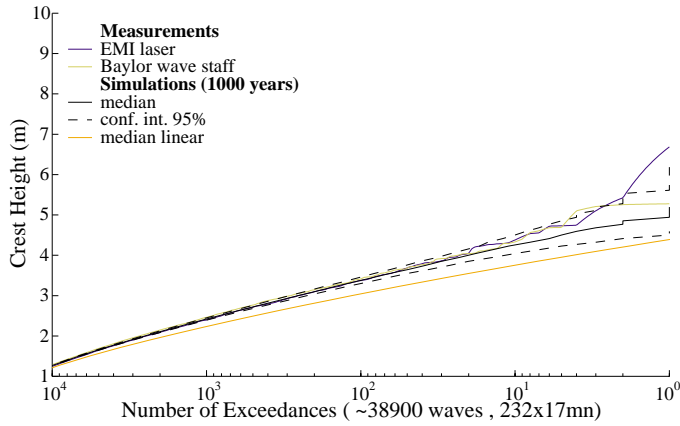


**Figure 6. EB Crest heights all-over campaign**

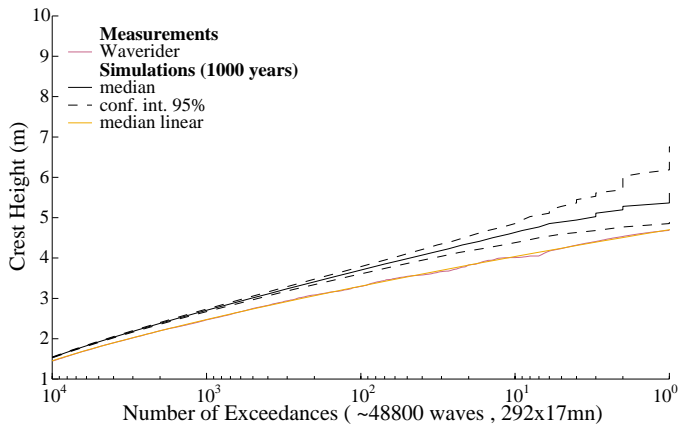


**Figure 7. Waverider Crest heights all-over campaign**

Since the high frequencies were poorly measured they have been filtered out of our comparisons. It is possible, however, that the some effect of the high frequency waves remains in the radar measurements due to their relatively large footprints. If a radar senses the highest point in its footprint and if the wavelength of the short waves is comparable to the size of the footprint, then the high frequency waves will be aliased into lower frequencies and not removed by the filter. We have not been able to confirm that the radars actually do sense the highest point in their footprints, so this explanation is still speculative.

More accurate measurement and simulation of wave components with frequencies above 0.64 Hz might possibly increase the crest height ratios slightly. For most purposes,

however, the difference would not be important since those components have very short wavelengths and thus do not affect engineering structures. Thus in the severe, but not extreme, sea states encountered during the campaign, we conclude that our second order model gives accurate predictions for the heights of crests.

It is instructive to note that the filtered trough depths are nearly identical for all of the sensors, as shown in Figure 8 for significant wave heights between 4.0 and 4.5 m. This fact has been strongly confirmed by the trough all-over campaign statistics. Apparently the sensors react differently to crests than to troughs.

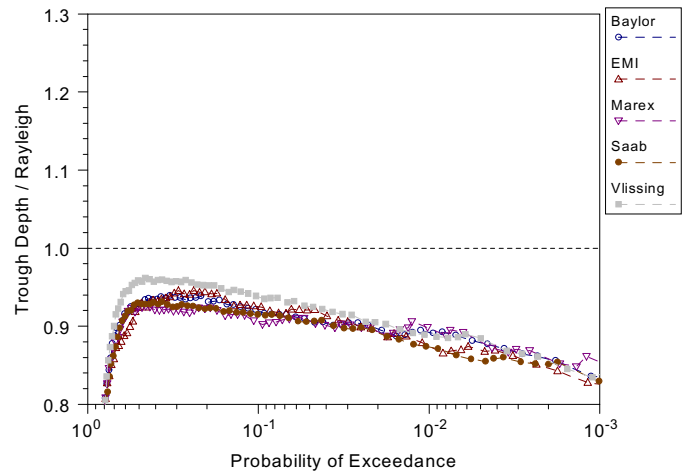


**Figure 8. Trough depth ratios, 4.0 < Hs < 4.5m**

## PARAMETRIC MODELS

As a better practical tool than simulations for engineering use, simplified parametric models have been proposed. Reinforced by the quality of the comparisons between measurements and 3D second order models, two new models have been recently proposed by the authors which take into account the 3D structure of the wave field. These models have been compared with previous theories and second order simulations.

### State of the art

**Rayleigh model.** When the sea surface elevation is considered to follow a Gaussian process model, the law of the local positive maxima given by Rice (1945) is

$$f_{\max>0}(\bar{x}) = \frac{1}{\sqrt{2\pi}} \left[ \varepsilon \exp\left(-\frac{\bar{x}^2}{2\varepsilon^2}\right) + I\bar{x} \exp\left(-\frac{\bar{x}^2}{2}\right) \int_{-\infty}^{\bar{x}/\varepsilon} \exp\left(-\frac{z^2}{2}\right) dz \right] \quad (15)$$

with  $\bar{x} = x/(\sqrt{m_0})$  the normalized amplitude and  $I = \sqrt{1-\varepsilon^2}$  an irregularity coefficient with  $\varepsilon = \sqrt{1-m_2^2/m_0m_4}$  a bandwidth parameter ( $m_i$  the spectral moments).

The distribution in Eq. (15) is not really useful for engineering purposes since it counts all of the small local maxima which can occur between zero crossings. Furthermore,

it depends on the fourth moment of the spectrum so it is very sensitive to the amount of energy at high frequencies. If  $\epsilon$  tends to 0 (narrowband), then local maxima become crest global maxima and so crest heights follow a Rayleigh law. In fact for high crest levels and the spectral bandwidth of actual seas the Rayleigh law given Eq. (16) approximates very well the maximum elevation between zero crossings of a Gaussian process.

$$P(C > c) = \exp\left(-8\frac{c^2}{H_s^2}\right) \quad (16)$$

The sea surface elevation is, however, obviously non Gaussian, and nonlinearities mainly due to the steepness of waves modify the crest heights. Other models have thus been proposed to give more accurate crest height distributions.

**Regular Stokes Waves.** In engineering design, crest heights are often estimated by taking the height and period of a individual wave at a specified probability level and then applying a high order regular wave theory to it. Stokes fifth order theory is commonly used for this purpose. Since such regular waves are often used as input to calculate forces on a structure, this method has the advantage of consistency. It has the disadvantage of neglecting the random and directionally spread nature of the real sea.

**Haring *et al.*** This model (Eq. (17)) is based on a nonlinear transformation of a Rayleigh law. The transformation is dependent of the crest height normalized by water depth  $d$ . It was first proposed by Jahns and Wheeler (1973) and fitted later using measurements by Haring *et al.* (1978). The fitting used wave staff measurements in the Gulf of Mexico and Waverider measurements in the North Sea, both in relatively shallow water. The model is thus not correct when  $d$  the water depth is infinite. In this case it tends to the Rayleigh law. The model is given by

$$P(C > c | H_s; d) = \exp\left(-8\frac{c^2}{H_s^2}\left(1 - 4.37\frac{c}{d}\left(0.57 - \frac{c}{d}\right)\right)\right) \quad (17)$$

**Derived Narrowband models.** Some other models were derived from a narrowband model of the 2D irregular second order wave model (Eq. (11)). If the envelope varies sufficiently slowly, the crest occurs at instant  $t_c$  when  $\Omega(t_c) = 0$ . Then the crest height given by the linear part is  $A(t_c)$ , and the crest height at second order is

$$A_{nonlin}(t_c) = A(t_c) + (T_{nb}^D(f_m) + T_{nb}^S(f_m))A^2(t_c) - T_{nb}^D(f_m)\frac{H_s^2}{8} \quad (18)$$

which links linear to nonlinear crest heights by a quadratic transformation:

$$C = C_{lin} + (T_{nb}^D(f_m) + T_{nb}^S(f_m))C_{lin}^2 - T_{nb}^D(f_m)\frac{H_s^2}{8} \quad (19)$$

Tayfun (1980), Tung and Huang (1986), Kriebel and Dawson

(1991), and Kriebel and Dawson (1993) proposed models based on such a nonlinear quadratic relation:

$$C = C_{lin} + \alpha(f_m; d)C_{lin}^2 + \beta = Q(C_{lin}) \quad (20)$$

and on the Rayleigh law for the distribution of the linear crests:

$$P(C_{lin} > c | H_s) = \exp\left(-8\frac{c^2}{H_s^2}\right) \quad (21)$$

So, in a classical way, the distribution of the nonlinear crests is obtained by applying the inverse nonlinear transformation Eq. (20).

$$P(C > c | H_s; f_m; d) = \exp\left(-8\frac{(Q^{-1}(c))^2}{H_s^2}\right) \quad (22)$$

The solution of the inverse transformation is Eq. (23) giving the distribution Eq. (24).

$$C_{lin} = Q^{-1}(C) = \frac{-1 + \sqrt{1 + 4\alpha(C - \beta)}}{2\alpha} \quad (23)$$

$$P(C > c | H_s; f_m; d) = \exp\left(-8\frac{\left(\frac{-1 + \sqrt{1 + 4\alpha(c - \beta)}}{2\alpha}\right)^2}{H_s^2}\right) \quad (24)$$

The differences between the models come from different choices of  $\alpha$ , and different approximations of  $Q^{-1}(C)$ . All the previous authors take  $\beta$  equal to zero and coefficient of the transformation Eq. (20) from second order regular Stokes wave. But unfortunately in finite water depth the irregular narrowband models do not tend to the regular model (Eq. (9))(due to the difference terms), making the Kriebel and Dawson finite depth model not an exact one. Tung and Huang (1986) made an error by taking into account in infinite water depth a low frequency part which in fact does not exist.

**Kriebel and Dawson.** The Kriebel and Dawson model is based on the second order regular Stokes wave model in infinite or finite depth, giving

$$C = C_{lin} + \frac{1}{2}\frac{R}{H_s}C_{lin}^2 \rightarrow C_{lin} = \left(-1 + \sqrt{1 + 2\frac{R}{H_s}C}\right)\frac{H_s}{R} \quad (25)$$

with

$$\begin{aligned} R &= k_m H_s f_2(k_m d) \\ k_m \leftarrow T_m &= 0.95 T_p \quad (\text{applying dispersion relation}) \\ f_2(k_m d) &= \frac{\cosh k_m d (2 + \cosh 2k_m d)}{2 \sinh^3 k_m d} - \frac{1}{\sinh 2k_m d} \end{aligned} \quad (26)$$

Kriebel and Dawson approximated the inverse transformation  $Q^{-1}(C)$ , first in 1991 at second order and later in 1993 with a corrected third order expansion. This induces a problem in the

crest distribution when the steepness is strong. These simplifications are not necessary as we know an analytic form of the inverse transformation Eq. (23). In the sequel of the report we will call the crest distribution based on Eqs. (25) & (26), the exact Kriebel model, and the model which uses the truncated inverse transformation the Kriebel model. The Kriebel model is given by:

$$C_{lin} = \left(1 - \frac{1}{2}R\frac{C}{H_s}\right)C \quad (27)$$

In infinite depth the exact Kriebel and Dawson model and the Tayfun model are the same. A difference could exist which comes from the definition of  $T_m$  Eq. (26).

$$P(C > c | (H_s, T_p)) = \exp\left(-\frac{8}{H_s^2 k_m^2}(-1 + \sqrt{1 + 2k_m c})^2\right) \quad (28)$$

### New models

Two new models have been recently proposed which take into account the 3D structure of the waves. The first one is a perturbed narrowband-derived model similar to those discussed in the previous section and the second one is a perturbed Weibull model.

**Prevosto model - Perturbed narrowband model.** Based on narrowband and infinite crested waves Eq. (24), this model uses the exact asymptotic narrowband transfer coefficients given in Prevosto *et al.* (2000). In order to take into account spectral bandwidth and directional spreading in Eq. (19), we consider the same model but with modified  $H_s$  and  $f_m$ .

$$\tilde{H}_s = \alpha_{H_s} H_s, \tilde{f}_m = \alpha_{f_m} f_m \quad (29)$$

In looking at different directional spectrum climatologies, including the WACSYS data base, and different water depths, the best  $\alpha_{H_s}$  and  $\alpha_{f_m}$  formulations have been determined from simulations and theoretical considerations to be:

$$\alpha_{H_s} = 1 - \frac{1}{2}(\tanh(k_m d) - 0.9) \sqrt{\frac{2}{1+s}} \quad (30)$$

$$\alpha_{f_m} = \frac{1}{1.23} \quad \text{with} \quad f_m = \frac{1}{T_{02}}$$

where  $s$  is the power of the equivalent  $\cos^{2s}$  directional distribution at the peak frequency (see Eq. (12)).

The formulation of  $\alpha_{H_s}$  has been chosen to take into account the fact that the effect of the directional spreading on the crest heights is opposite in deep and shallow water (Prevosto (1998)). This model has the advantage of furnishing a unique expression both the 2D and 3D cases, and so can be adapted to all intermediate situations.

**Forristall model - Perturbed Weibull model.** This model is based on a Weibull law with the two parameters written as

polynomials in the steepness and Ursell number.

$$P(C > c) = \exp\left(-\left(\frac{c}{\alpha H_s}\right)^\beta\right) \quad (31)$$

$$\alpha = \alpha_1 + \alpha_2 S_1 + \alpha_3 U_r$$

$$\beta = \beta_1 - \beta_2 S_1 - \beta_3 U_r + \beta_4 U_r^2$$

$$S_1 = \frac{2\pi H_s}{g T_{01}^2} \quad \text{steepness} \quad (32)$$

$$U_r = \frac{H_s}{k_{01}^2 d^3} \quad \text{Ursell number}$$

Starting from simulations based on a synthetic directional spectrum data base and different water depths, two different sets of coefficients of the polynomials were fitted from 2D and 3D simulations (Forristall (2000)).

$$\mathbf{2D} \quad \alpha = 1/\sqrt{8} + 0.2892S_1 + 0.1060U_r \quad (33)$$

$$\beta = 2 - 2.1597S_1 + 0.0968U_r^2$$

$$\mathbf{3D} \quad \alpha = 1/\sqrt{8} + 0.2568S_1 + 0.0800U_r \quad (34)$$

$$\beta = 2 - 1.7912S_1 - 0.5302U_r + 0.284U_r^2$$

The advantage of this model is its simplicity. Of course it does not take into account variations in the directional spreading, but as it will be shown hereafter, it works well when facing realistic wind sea directional spreading.

### Inside sea states comparison

These two models have been compared using a simulated data base starting from the directional spectrum data base of the WACSYS project. Three water depths were used. They were infinite water depth, 30 meters water depth and the actual water depth of the WACSYS site. In Figs. 9-12, each colored line corresponds to the error between the crest heights given by the parametric model and those obtained from simulations at the same level of probability. The plotted error could be written

$$\text{error}(c) = F_C^{-1}(\hat{F}_C(c)) - c \quad (35)$$

where  $F_C(c)$  is the distribution of crest heights given by the parametric model and  $\hat{F}_C(c)$  is the empirical distribution of crest heights estimated from 1000 one hour time series, corresponding to one directional spectrum and one water depth. All the 3 water depths times 100 sea states lines have been superimposed. Note that the scales of the figures differ.

As is well known the Rayleigh model always underestimates the crest heights (Fig. 9). The error in this data set reaches 80 cm. When using the narrowband model, corresponding to  $s = \infty$  in Eq. (30), the error is decreased to a range from -15 cm. to 17 cm. (Fig. 10). The two new models, which take account of the directional spreading reduce again the range of

the error by a factor two, -8 cm to 8 cm for the Prevosto model (Fig. 11) and -9 cm to 6 cm for the Forristall model (Fig. 12).

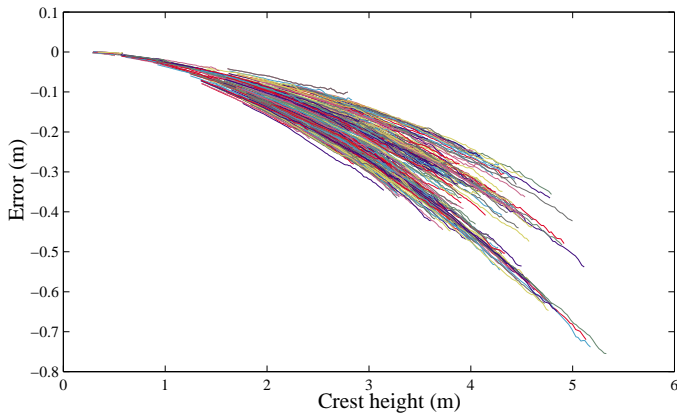


**Figure 9. Model vs. empirical, Rayleigh model**

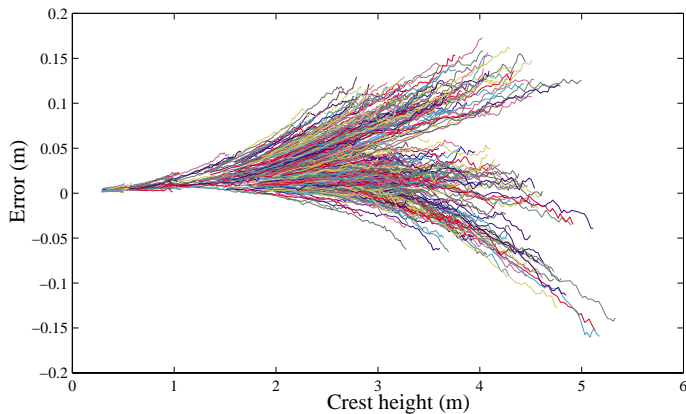


**Figure 10. Model vs. empirical, Narrowband model**

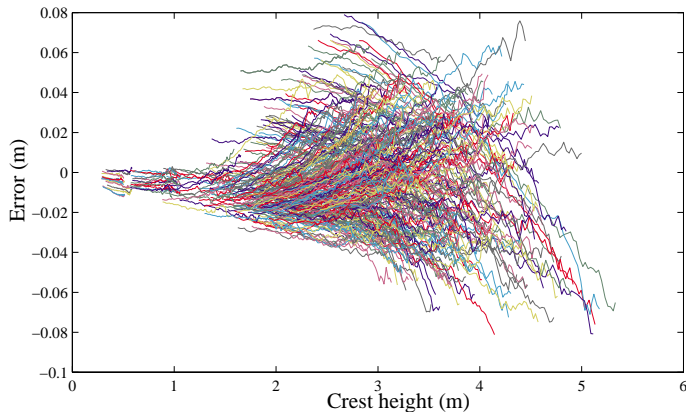


**Figure 11. Model vs. empirical, Prevosto model**

### All-over campaign comparison

Another comparison has been made in using the number of exceedances all-over the campaign. For each parametric model we follow the different steps:

- choose a water depth: 1000 m., 30 m., WACSIS site water depths 17-20 m.

- take a directional spectrum of the WACSIS data base and calculate parameters of the model ( $H_s$ ,  $T_{02}$ ,  $T_{01}$ ,  $s$ )
- calculate the number of waves  $N$  during one hour of this sea state by  $3600/T_{02}$  and then calculate the number of exceedances by multiplying the number of waves by the probability of exceedance given by the model,  $N \cdot P(C > c)$
- cumulate with the previous sea states

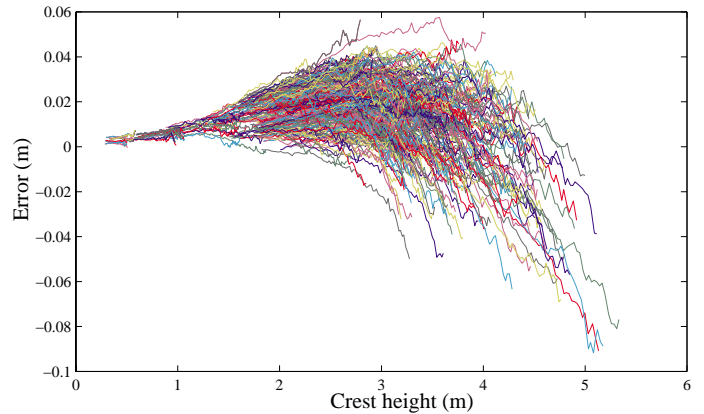


**Figure 12. Model vs. empirical, Forristall model**

For the simulations:

- choose a water depth: 1000 m., 30 m., WACSIS site water depths 17-20 m.
- take a directional spectrum of the WACSIS data base and simulate 1000 one hour time series
- calculate the number of exceedances and divide it by 1000 to obtain the mean number of exceedance an hour.
- cumulate with the previous sea states

The results are given in Figs 13-15. In “shallow” water (17-20 m.) (Fig. 13), the Kriebel model is completely wrong, the Haring and exact Kriebel models overestimate the heights, and Prevosto and Forristall models are very close to the simulations. In intermediate water depth (30m) (Fig. 14), in decreasing order the Kriebel, Haring and exact Kriebel models overestimate and the Prevosto and Forristall models agree with the simulations. In deep water (Fig. 15), all the models are very close to the simulations apart from the Haring model which gives exactly the same results as the Rayleigh model as has been explained previously.

### Simulations vs. parametric models - Conclusion

Apart from the infinite water depth situation for the exact Kriebel model, the parametric models of crest distributions which were proposed in the past are not very accurate. The two new parametric models which have been proposed by the authors give results very close to what is obtained empirically from second order 3D irregular simulations of the WACSIS directional spectra, whatever the water depth.

The formulation of the Forristall model is simpler than the Prevosto model but it does not take into account explicitly the

directional spreading as the Prevosto model does. So the Prevosto model will be more accurate in extreme directional spreading situations (very short-crested or close to swell situations).

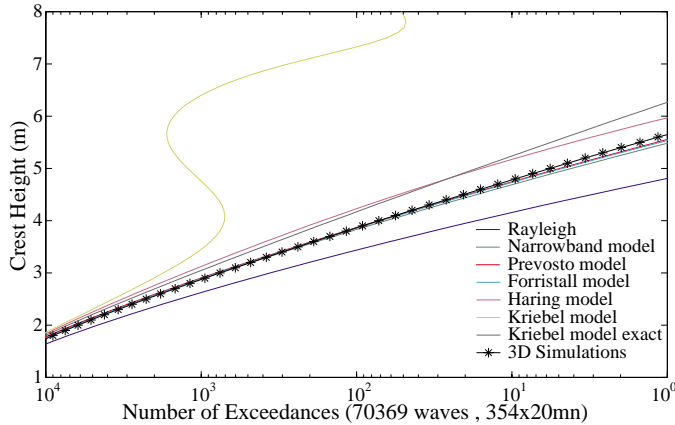


**Figure 13. Models vs. empirical, WACSIS site water depths 17-20 m**

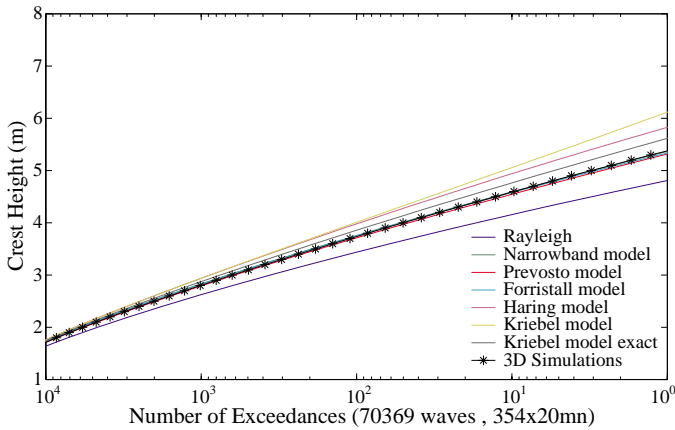


**Figure 14. Models vs. empirical, water depth 30 m**

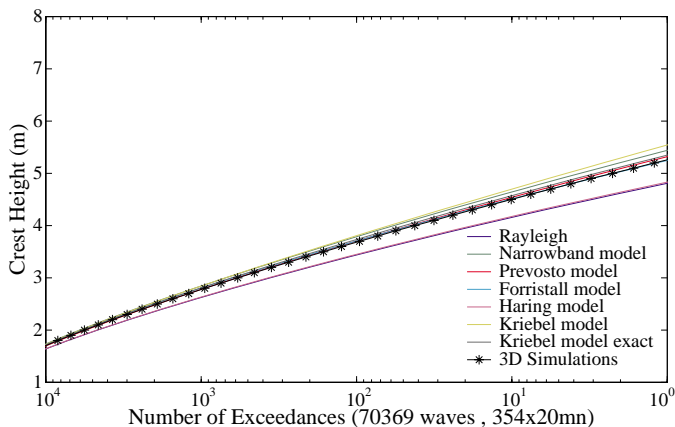


**Figure 15. Models vs. empirical, water depth 1000 m.**

#### ACKNOWLEDGMENTS

The WACSIS JIP was supported by Amoco Corp., BP Exploration Operating Company Limited, Chevron Petroleum

Technology Company, Conoco, Den Norske Stat Oljeselskap, Health and Safety Executive, Ifremer, Marathon Oil Company, Mobil Technology Company, Saga Petroleum ASA, Shell International Deepwater Services B.V. and Texaco Group Inc. Since the project began, several of the supporting companies have merged or changed names.

#### REFERENCES

Chen, L., Zhang, J., 1994, "On interaction between intermediate-depth long waves and deep-water short waves", *Offshore Technol. Res. Center Report*, no. A5575, p. 37.

Forristall, G. Z., Barstow, S. F., Krogstad, H. E., Prevosto, M., Taylor, P. H., Tromans, P., 2002, "Wave Crest Sensor Intercomparison Study: An Overview of WACSIS", *Proceedings, 21st International Conference on Offshore Mechanics and Arctic Engineering*, Oslo, OMAE 28438.

Forristall, G.Z., 2000, "Wave Crest Distributions: Observations and Second-Order Theory", *Journal of Physical Oceanography*, vol. 30, no.8, pp. 1931-1943.

Forristall, G.Z., 1978, "On the statistical distribution of wave heights in a storm", *Journal of Geophysical Research*, no. 83, pp. 2353-2358.

Haring, R.E., Heideman, J.C., 1978, "Gulf of Mexico rare wave return periods", *Proc. Offshore Technology Conference*, pp. 1537-1550, OTC 3230.

Jahns, H.O., Wheeler, J.D., 1973, "Long-term wave probabilities based on hindcasting of severe storms", *J. Pet. Technol.*, pp. 473-486.

Kriebel, D.L., Dawson, T.H., 1991, "Nonlinear effects on wave groups in random seas", *J. Offshore Mech. Arctic Eng.*, no. 113, pp. 142-147.

Kriebel, D.L., Dawson, T.H., 1993, "Nonlinearity in wave crest statistics", *Proc. 2nd Int. Symp. Ocean Wave Measurement and Analysis*, pp. 61-75.

Longuet-Higgins, M. S., 1963, "The effect of non-linearities on statistical distributions in the theory of sea waves", *J. Fluid Mech.*, vol. 17, pp. 459-480.

Prevosto, M., 2000, "Statistics of wave crests from second order irregular wave 3D models", *Proc. Rogue Waves 2000*, pp. 59-72.

Prevosto, M., Krogstad, H. E., Robin, A., 2000, "Probability distributions for maximum wave and crest heights", *Coastal Engineering*, vol. 40, pp. 329-360.

Prevosto, M., 1998, "Effect of Directional Spreading and Spectral Bandwidth on the Nonlinearity of the Irregular Waves", *Proc. 8th ISOPE Conf.*, vol. III, pp. 119-123.

Rice, S.O., 1945, "Mathematical analysis of random waves", *Bell Syst. tech. J.*, vol. 24, pp. 46-156.

Rychlik, I., Johannesson, P., Leadbetter, M.R., 1997, "Modeling

and statistical analysis of ocean-wave data using transformed Gaussian processes", *Marine Structures*, vol. 10, pp. 13-47.

Sharma, J. N., Dean R. G., 1979, "Development and evaluation of a procedure for simulating a random directional second order sea surface and associated wave forces", *Ocean Engineering Report*, no. 20, University of Delaware, Newark.

Tayfun, M. A., 1980, "Narrow-band nonlinear sea waves", *J. Geophys. Res.*, vol. 85, no. C3, pp. 1548-1552.

Tromans, P. S., Taylor, P. H., 1998, "The shapes, histories and statistics of non-linear wave crests in random seas", *Proc. OMAE Conf.*, OMAE-981206.

Tromans, P. S., 2002, "A spectral response surface method for calculating crest elevation statistics", *Proc. 21st International Conference on Offshore Mechanics and Arctic Engineering*, Oslo, OMAE 28535.

Tung, C.-C., Huang, N. E., 1985, "Peak and trough distributions of nonlinear waves", *Ocean Eng.*, vol. 12, no. 3, pp. 201-209.

Zhang, J., Chen, L., Ye, M., Randall, R. E., 1996, "Hybrid wave model for unidirectional irregular waves, Part I. Theory and numerical scheme", *Appl. Ocean Res.*, vol. 18, nos 2-3, pp. 77-92.

Zhang, J., Yang, J., Wen, J., Prislun, I., Hong, K., 1999, "Deterministic wave model for short-crested ocean waves: Part I. Theory and numerical scheme", *Applied Ocean Research*, vol. 21, no. 4, pp. 167-188.